Hemispheric Daytime Ionospheric Response To Intense Solar Wind Forcing

A. J. Mannucci, Bruce T. Tsurutani, Byron Iijima, Attila Komjathy, Brian Wilson, Xiaoqing Pi, Lawrence Sparks, George Hajj, Lukas Mandrake

Jet Propulsion Laboratory, California Institute of Technolog, Pasadena, California

Walter D. Gonzalez

Instituto Nacional de Pesquisas Espaciais, São José dos Campos, SP, Brazil

Janet Kozyra

University of Michigan

K. Yumoto

Space Environment Research Center, Kyushu University, Japan

M. Swisdak

Icarus Research, Inc., Bethesda, Maryland

J.D. Huba

Plasma Physics Division, Naval Research Laboratory, Washington, DC

R. Skoug

Los Alamos National Laboratory, Los Alamos, New Mexico

We investigate the ionospheric response to events where the z-component of the interplanetary magnetic field, B_z, becomes large and negative for several hours, associated with the largest geomagnetic storms over the prior solar maximum period (2000-2004). We compute the average vertical total electron content (TEC) in the broad region covering 1200-1600 local time and ±40 degrees geomagnetic latitude (dipole), using data from the global network of Global Positioning System (GPS) receivers. In several cases, we find approximately a two-fold increase in total electron content within 2-3 hours of the time when the southward-B_z solar wind impinged on the magnetopause. We also analyze daytime super-satellite TEC data from the GPS receiver on the CHAMP satellite orbiting at approximately 400 km altitude, and find that for the October 30, 2003 storm at mid-latitudes the TEC increase is nearly one order of magnitude relative to the TEC just prior to the B_z southward onset. The geomagnetic storm-time phenomenon of prompt penetration electric fields into the ionosphere from enhanced magnetospheric convection is the most likely cause of these TEC increases, at least for certain of the events, resulting in eastward directed electric fields at the equator. The resulting dayside vertical **ExB** drift of plasma to higher altitudes, while solar photons create more plasma at lower altitudes, results in a "daytime super-fountain" effect that rapidly changes the plasma structure of the entire dayside ionosphere. This phenomenon has major practical space weather implications.

1. INTRODUCTION

It is well known that the interaction between southward interplanetary magnetic fields (IMFs) and the Earth's magnetic field leads to strong dawn-to-dusk electric fields in the magnetosphere and an overall increase in magnetospheric convection. This convection, in turn, causes intense ring current buildup and magnetic storms [*Gonzalez and Tsurutani*, 1987; *Gonzalez et al.*, 1994; *Kozyra et al.*, 1997; *Kamide et al.*, 1998]. This rapid change in magnetospheric conditions can have dramatic effects on the Earth's ionosphere. If electric fields can penetrate to the low latitude ionosphere before shielding builds up [*Tanaka and Hirao*, 1973], they can modify equatorial ionospheric electrodynamics. Resulting eastward electric fields in the daytime will cause upward **E**x**B** drift in the equatorial ionosphere during the day. This paper concerns the ionospheric effects of electric fields associated with geomagnetic disturbances.

In this paper we analyze data from several intense interplanetary events characterized by strong southward (negative B_Z in GSM coordinates) interplanetary magnetic field, and measure the ionospheric consequences during the initial phase of the magnetic storm. We report that at the equator and middle latitudes, significant increases in ionospheric total electron content (TEC) occur, as measured by dual-frequency Global Positioning System (GPS) receivers (*Mannucci et al.*, 1998; *Mannucci et al.*, 1999). Little is presently reported about the full hemispheric dayside response to intense magnetic storms.

Significant changes in TEC can be produced soon after event onset by intense disturbance-related electric fields originating from the magnetosphere-ionosphere interaction. Disturbance electric fields at low latitudes have been identified principally from two causes, as: (a) prompt penetration zonal electric field often observed in the equatorial latitudes [*Sastri*, 1988; *Fejer and Scherliess*, 1995; *Abdu et al.*, 1995; *Sobral et al,.* 1997; *Sobral et al.,* 2001; *Fejer*, 2002; *Sastri et al.*, 2002; *Kelley et al.*, 2003; *Vlasov et al.*, 2003] and/or (b) delayed electric fields produced by the disturbance dynamo driven by modified thermospheric winds due to energy input at high latitudes [*Blanc and Richmond*, 1980; *Richmond and Lu*, 2000; *Scherliess and Fejer*, 1997]. Zonal electric fields from these two causes, depending on their polarity and duration, could cause large uplifts or downdrafts of the ionospheric plasma leading to large-scale local-time dependent enhancements or decreases of the vertical TEC.

Electrodynamics that occurs in daytime is especially important because the ionospheric plasma is highly responsive to such disturbance electric fields, and the daytime is where the quantity of terrestrial plasma is largest. GPS observations suggest that large quantities of plasma are generated rapidly (within 2-3 hours) in the equatorial region through mid-latitudes, possibly affecting the amount of plasma entering higher latitudes. A suggestive picture of full hemispheric response is shown in Figure 1. A global network of GPS receivers has been used to estimate vertical total electron content along the lines of sight between each receiver and several GPS satellites in view simultaneously (typically 6-10). The map shows the measured average TEC, obtained at a 30-second cadence, between UT 2100 and 2115 for October 29, 2003. Over North America, an enhanced narrow plume of plasma can be seen stretching from middle to high latitudes in the mid-afternoon sector. Vertical TEC data from a low-Earth orbiting GPS receiver, which has no data gaps over the oceans, suggests that in the early afternoon large TEC increases have occurred spanning the entire low-to-middle latitude ionosphere. The existence of this large "plasma pool" may contribute to the large TEC gradients associated with the plume.

These hemispheric-scale plasma increases have important practical consequences. There are many applications for which large TEC gradients, and associated instabilities, are major concerns, including to radar, communications and GPS-based navigation systems, including those used by the Federal Aviation Administration (FAA) for civil aircraft navigation. The fact that plasma gradients at mid-latitudes can be enhanced by plasma uplift spanning the low-to-midlatitude dayside hemisphere is important for predictive purposes and for understanding the magnitude and temporal evolution of significant gradients in TEC at mid-latitudes. The performance of the FAA's system is limited by incomplete scientific understanding of low-through-middle latitude plasma response.

In this paper we will address the problem of the dayside ionospheric response to intense solar wind forcing, using measurements provided by the Global Positioning System (GPS) from ground and space-borne receivers. A companion paper [*Tsurutani et al.*, 2004b] analyzed the November 6, 2001 event in detail using multiple observations.

In this paper, we explore the general phenomenon of prompt TEC increases after B_z southward turnings in the solar wind for a number of events. The data tend to support the hypothesis that, in the early phases of intense geomagnetic storms, B_z southward turning is often associated with significant daytime TEC increases. Whether these are all related to a similar cause is a matter of future research.

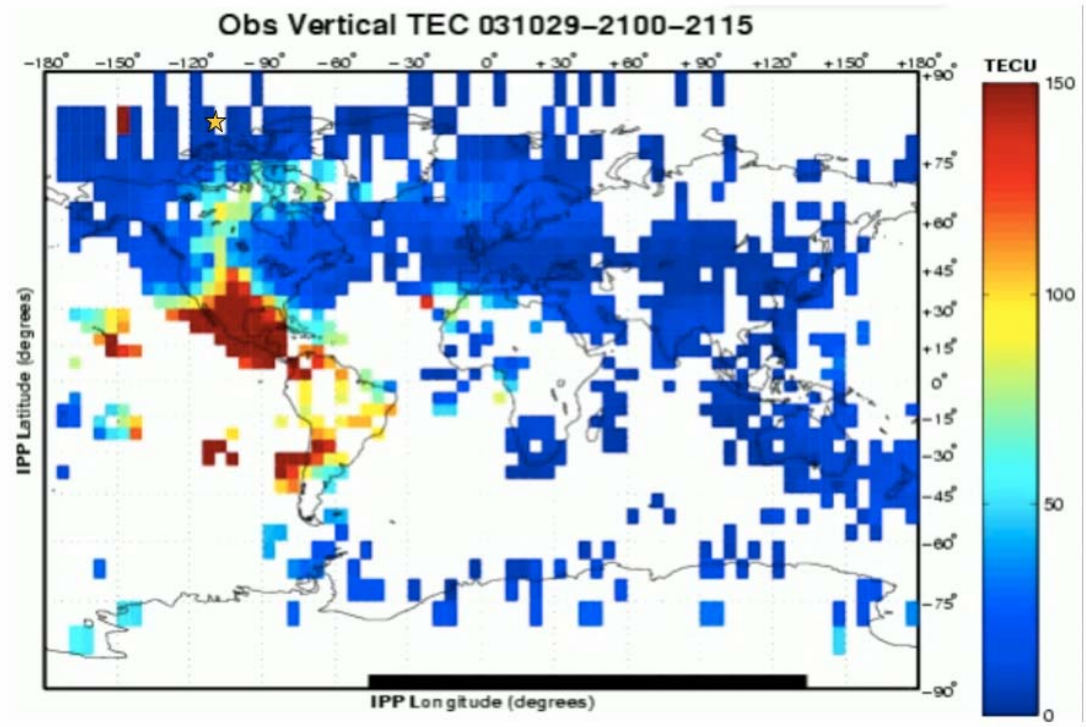

Figure 1: A global "snapshot" of vertical total electron as measured by a global network of GPS receivers on October 29, 2003 from 2100-2115 UT when a geomagnetic storm was in progress. A plasma tongue structure extending to high latitudes is visible in North America, which may be dependent on enhanced plasma generation at low latitudes due to disturbance electric fields. A star indicates the geomagnetic pole location. Units: 1 TECU = 10^{16} electrons/m^2.

2. DATA ANALYSIS AND METHOD

Our measurements of the column density of electrons, referred to as total electron content (TEC), were obtained from the Global Positioning System (GPS) satellite signals as received by both ground-based receivers (~200 distributed around the globe) and a receiver onboard the CHAMP satellite in low-Earth orbit at approximately 400 km altitude. The locations of both the satellites and receivers are known to a few decimeters or better, and since straight line propagation is essentially correct for the signals, the electron content is measured along a geographically well-located line-of-sight between GPS satellite and receiver.

A schematic of the TEC measurement geometry is shown in Figure 2. There are approximately 28 GPS satellites located in circular Earth orbit at an altitude of 20,200 km. For simplicity, only one GPS satellite is illustrated in the figure. Each receiver simultaneously tracks multiple (4-10) GPS satellite signals. The relative delay between the two GPS transmission frequencies L1 (1575 GHz) and L2 (1227 GHz) is directly related to the column density of electrons (total number of electrons per unit area) along the line of sight [*Mannucci et al.*, 1999; *Mannucci et al.*, 1998].

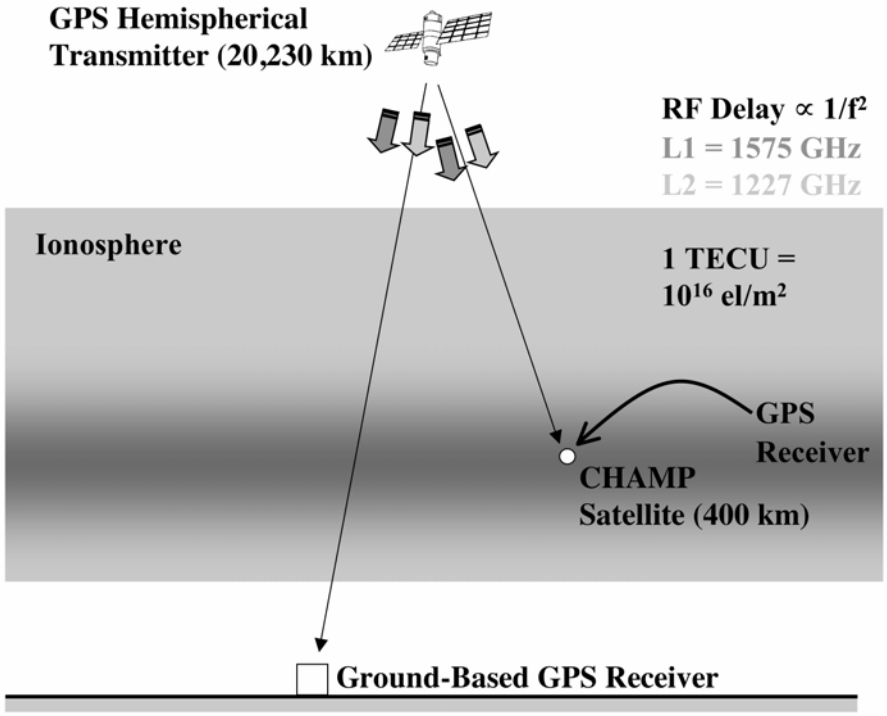

Figure 2: A schematic of a GPS satellite transmitter and low altitude satellite and ground-based GPS receivers. The GPS satellites broadcast continuous transmissions at two frequencies f (L1 and L2). Signal processing is used to extract ionospheric electron density structure (total electron content) towards multiple satellites in view simultaneously. The shaded area represents the ionosphere.

The CHAMP satellite (*Reigber et al.*, 2002) possesses a GPS receiver and zenith viewing antenna that tracks all GPS satellites in view at positive elevation angles. CHAMP is in a polar orbit (87° inclination) at a slowly declining altitude of ~400-430 km over the period of this study, with an orbital period of approximately 100 minutes. Data for elevation angles within 70º of the vertical, or higher, were used exclusively in this study. Otherwise no other data deletions have been performed. To normalize the measurements obtained at multiple elevation angles, the slant TEC data have been used to estimate the vertical TEC directly above the low-Earth orbiter (LEO), assuming a simple geometrical factor that accounts for the difference between slant and vertical TEC. We assume the vertical distribution of density is a spherical shell ionosphere of uniform (horizontally stratified) density, 700 km-thick, above the CHAMP altitude. For elevation angles greater than 30º as used in this study, the error from this simplifying assumption is not a significant factor for our analysis, as suggested in a later section.

The ground-based GPS data set used is composed of ~100 stations from the International GPS Service data centers [*Moore*, 2001]. The obliquity function used to estimate the vertical TEC from the slant observations is computed modeling the ionosphere as a spherical slab of uniform electron density between 450 and 650 km altitude. The latitude and longitude at which the ground-to-satellite line-of-sight intersects the ionosphere is computed using a spherical shell at 450 km altitude. Detailed discussion concerning the removal of instrumental offsets for both ground-based receivers and satellite-based receivers is beyond the scope of this paper. If the reader is interested in further information on the topic of extracting TEC measurements from ground-based GPS receivers, see *Mannucci et al.* [1999].

We use Level 2 data from the ACE satellite upstream of the Earth (GSM position x,y,z = 1.4 x 10^6 km, 1.2 x 10^5 km, -2.0 x 10^5 km) to provide the estimates of the B_z southward turning onset times that initially cause the geomagnetic disturbance, and hourly *Dst* geomagnetic data from the National Geophysical Data Center to monitor the total intensity of the resulting geomagnetic storm.

3. November 6, 2001 Storm

The event of November 5-6 2001 is analyzed first, following the detailed discussion in Tsurutani *et al.*, 2004b. Measured parameters pertaining to the event are shown in Figure 3. The top two panels are interplanetary parameters taken by the ACE spacecraft located at 1.4 x 10^6 km upstream of the Earth. They are: the solar wind speed and z-component of the magnetic field B_Z (GSM coordinates). Using the measured solar wind speed of ~700 km/s, a

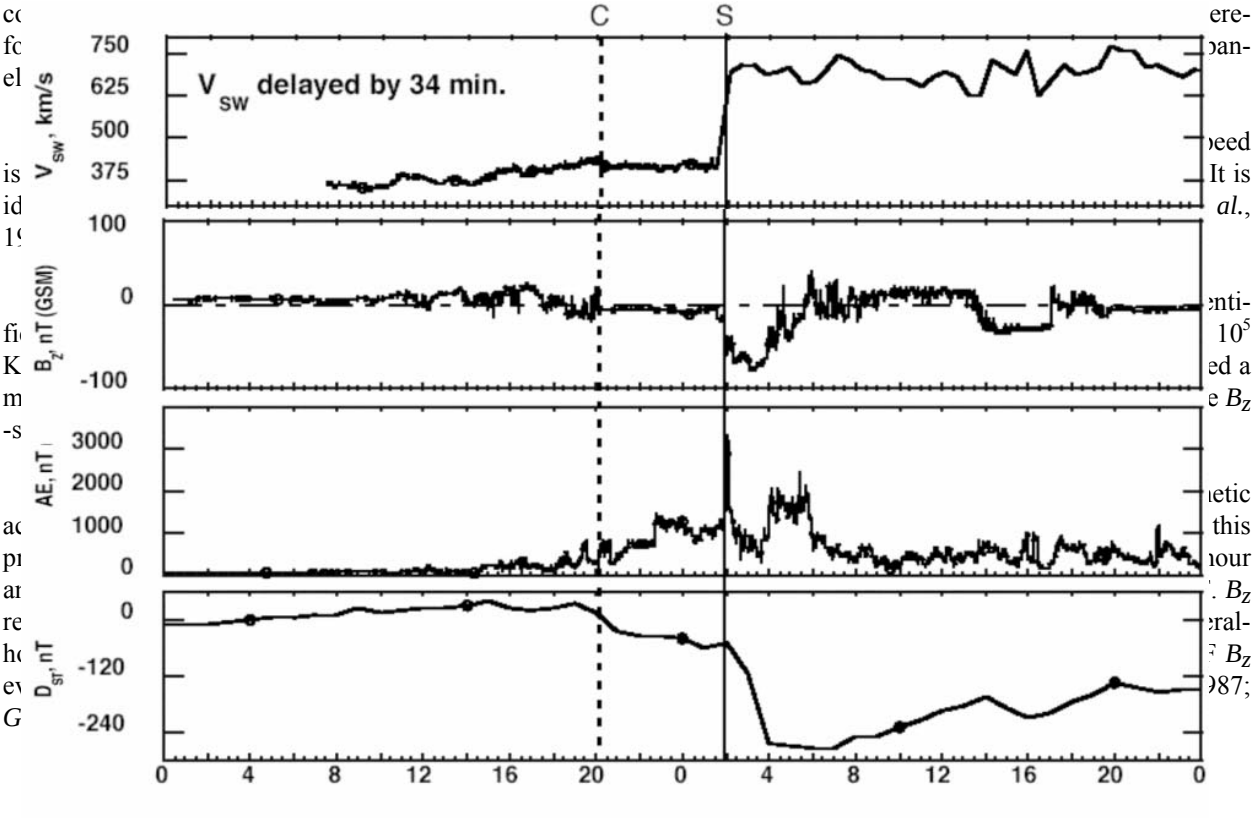

Figure 3: The interplanetary event of 5-6 November 2001. The interplanetary data is taken by the ACE spacecraft. The magnetic field is plotted in GSM coordinates. The time delay of the solar wind and magnetic field convection from ACE to the magnetopause is ~34 min. Thus the interplanetary shock should impinge upon the magnetosphere at ~0154 UT. A strong dawn-to-dusk electric field is imposed on the magnetosphere at this time. An AE ~ 3000 nT substorm onset and a magnetic storm reaching a magnitude of *Dst* = -275 nT also start at the time of the shock arrival.

For the remainder of the paper, we will discuss the impact of sudden intense interplanetary electric field (IEF) on the Earth's ionosphere (IEF = $V_{SW} \times B_Z$). This electric field onset occurs at ~0120 UT at ACE and assuming a time shift of 34 minutes, it should have been imposed on the magnetosphere at ~0154 UT. It should also be remembered that there is a small but important "precursor" interplanetary electric field associated with the negative B_Z (due to the slow magnetic cloud ahead of the shock) and a concomitant moderate storm, occurring prior to the shock electric field event. For other events discussed in this paper, the onset time of the southward B_Z turnings, shifted in time according to the measured solar wind speed, are used to assess the correspondence between changes in magnetospheric convection and ionospheric modification.

A synoptic view of the dayside TEC response to the interplanetary shock is available from ground-based TEC measurements as shown in Figure 4. The data are plotted as a function of local time and magnetic latitude. Figure 4a (top panel) shows November 4, 2001 quiet-time "baseline" data from 0409 to 0456 UT two days before the interplanetary event. Each colored point in the figure represents an estimate of vertical TEC from a link between a GPS

ground receiver and a GPS satellite. About ten data epochs are recorded along each satellite-receiver link during the 45-minute period of the map. Each receiver tracks numerous satellites, typically a number between four and ten, at every epoch. Estimates of the TEC above the CHAMP satellite track from an altitude of 430 km, at approximately 1900-2000 local time (LT) over most latitudes, are superposed.

Figure 4a shows a typical pattern of global TEC, that reaches a maximum on the dayside due to solar UV and X-ray irradiation, and is centered at approximately 1400 local time. The area of TEC values exceeding 100 TECU, the red area, extends from -34^{o} MLAT to $+20^{o}$ MLAT. The bias towards southern latitudes is typical for northern wintertime (November) due to the influence of the prevailing circulation from south-to-north.

Figure 4b shows the TEC distribution after the shock event on 6 November 2001, from 0414 to 0500 UT (~2 to 3 hours after the shock). The post-shock TEC distribution is markedly different from the quiet-time distribution: the region of enhanced TEC (> 100 TECU) is much larger ranging from $+48^{o}$ MLAT to -40 MLAT. The westward and eastward extent of the red areas is approximately the same pre- and post-shock: ~0900 to ~2100 LT.

From a detailed comparison (not shown) of Figures 4a and 4b at 14 LT, where the maximum TEC occurs at low latitudes, it is noted that on 6 November the ground-based TEC has increased from ~145 TECU (4 November) to ~170-180 TECU. Thus, there is an absolute increase in TEC at this local time by ~21%. Figures 4a and 4b also contain the CHAMP upward viewing TEC data obtained at dusk. The TEC values above CHAMP are the same as those above the ground within an uncertainty of 10%. Thus, at ~1900 LT, nearly all of the ionospheric plasma is above ~430 km altitude.

TEC increases can be caused by eastward-directed electric fields causing plasma uplift to altitudes of reduced recombination rate (see *Tsurutani et al.* 2004b, and references therein; also *Tanaka and Hirao*, 1973). The relatively early ionospheric response for this event suggests that the mechanism for the electric fields is prompt penetration, as opposed to thermospheric dynamo. Data that tends to corroborate the prompt electric field mechanism is shown in Figure 5, an estimate of the equatorial electrojet (EEJ) current strength using magnetometer data. The east-west flowing EEJ is an indirect measure of eastward-directed electric fields during daytime, since the intensity of the EEJ depends on vertical **ExB** drift velocity through the intermediate mechanism of vertically-directed polarization fields (Anderson et al. 2002; Rastogi and Klobuchar, 1990). Figure 5 shows the equatorial electrojet current intensity over the Pacific equatorial station Yap (9.3º N, 138.5º E, dip angle: -0.6º), which was obtained by subtracting the diurnal range of the horizontal (northward) component of magnetic field intensity (ΔH) over a non-EEJ station Guam (13.58º N, 144.87º E, dip angle: 9º) from that of Yap. Although the EEJ estimate cannot be compared directly to the IEF magnitudes, it is clear that excellent agreement exists for the temporal trends comparing the ground-based and satellite-based data (ACE).

During the interplanetary shock event and consequential storm, Yap was in the midday sector. The large increase of the EEJ intensity over the Pacific sector (blue trace) coincident with the shock arrival time ("S" in the figure) is consistent with a large disturbance penetration electric field of eastward polarity produced on the dayside by the shock event. The interplanetary electric field is superposed on this figure (calculated from the data in Figure 3 but at a cadence of 30 minutes) and shows a pattern similar to that measured at the equator (for another example of EEJ correlation to solar wind, see Kelley et al., 2003).

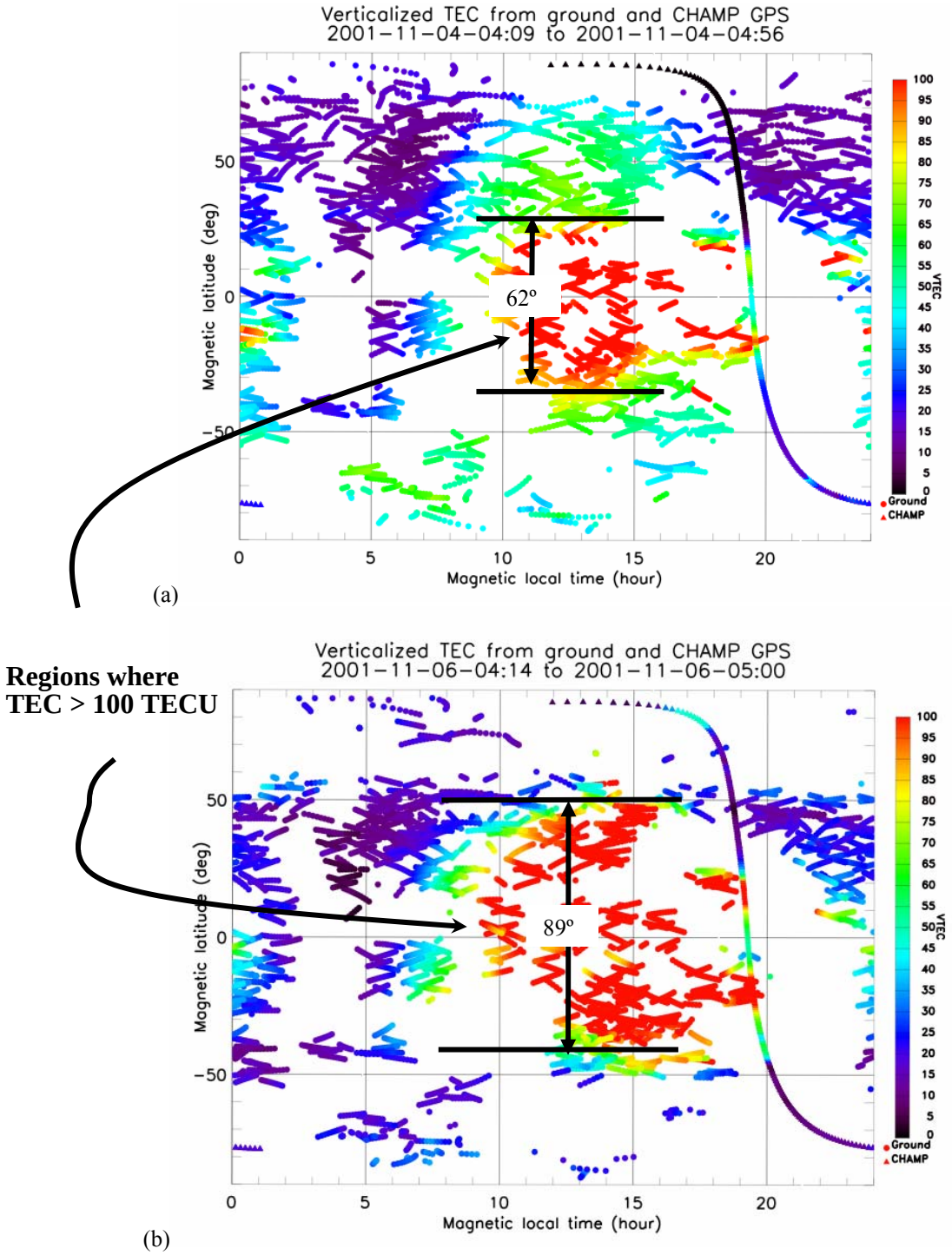

Figure 4: The ~100-station ground-based TEC data for 4 November from 0409 to 0456 UT (background) in panel (a) and for 6 November from 0414 to 0500 UT (post shock event) in panel (b). Integrated electron content data above CHAMP altitude of 430 km are also shown (to the same intensity scale). The dayside post-shock region of enhanced TEC (> 100 TECU) is much broader in latitudinal extent, ranging from +48 ^{o} MLAT to -40 ^{o} MLAT, compared to the range 28º → –34º for the region where TEC > 100 TECU on the quiet day.

An eastward disturbance electric field at daytime through dusk is consistent with *Nopper and Corovillano* [1978], which contains a calculation of equatorial electric field direction when Region 1 field aligned currents are much larger than Region 2 currents (under-shielding) assuming an average ionospheric conductance pattern. (See also *Senior and Blanc*, 1984; *Spiro et al.*, 1988; *Fejer et al.*, 1990). It is clear from Figure 5 that a large electric field, as inferred via magnetometer data, tracks the pattern of IEF onset and decay. This is suggestive of penetration electric fields, as opposed to other causes (see also Kelley et al., 2003). The analysis of multiple events in the next section, and the fact that TEC increases are always observed following soon after the large B_Z southward event, suggests that the prompt penetration mechanism is a major contributor to the hemispherical dayside plasma redistribution.

4. Multi-Event Analysis

The November 6, 2001 event was studied in great detail in Tsurutani *et al.*, 2004b. A conclusion of that work was that the TEC changes were due to eastward-directed electric fields at the equator that appeared immediately after the shock reached the magnetopause. The **ExB** plasma drift associated with this eastward electric field will lift the ionospheric plasma to higher altitudes where recombination rates are low, thereby reducing the average loss (recombination) rate of ionospheric plasma. Solar UV radiation will form new electron-ion pairs at lower altitudes, leading to major increases in TEC that is the major focus of this paper. In this section, we will look at a number of interplanetary events of similar structure to assess the dayside TEC response.

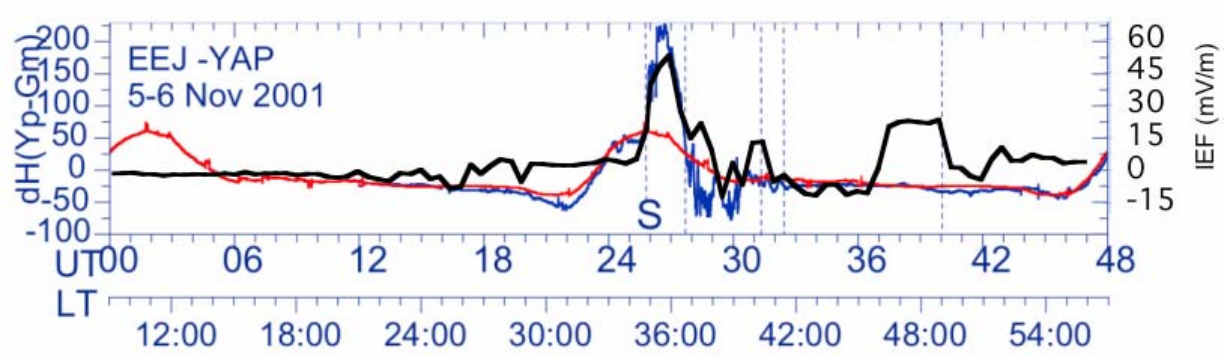

Figure 5: The Equatorial Electrojet –EEJ current intensity over the Yap magnetometer station in the midday sector is shown. The reference day curve for Yap (in red) is taken from 5 Nov. The starting time in the figure is 00 UT 5 Nov. The LT at Yap (UT plus 9 hrs) is shown at the bottom. Vertical line 1 indicates the onset of the shock. Shown in black is the interplanetary electric field ($V_X B_Z$) time shifted at each point according to the velocity measured at ACE and assuming a distance to ACE of 1.4×10^6 km. The adjusted curve was subsequently shifted as a whole to line up with the blue curve.

We are interested in the temporal behavior of daytime TEC before, during and after a number of candidate events leading to intense geomagnetic storms. We compute a time series of average TEC in a fixed local-time/latitude region using data from a global network of ~100 GPS receivers. The coverage of the network is extensive enough that some data exists in the prescribed local time region at all universal times, although the number of points (coverage) varies with time, as does the latitude/longitude distribution of sites. For this reason, we plot the averages for two days preceding the storm day to reveal the quiet time variability solely due to changing coverage and natural ionospheric variability. As in the previous section, an obliquity function is used to estimate the vertical TEC from the slant TEC measurements obtained above 10 degrees elevation angle. The ionospheric pierce point location is used to select data included in the average.

Figure 6 shows the TEC averages for the local time range 1200-1600 LT and magnetic latitude range ±40 degrees (dipole) every 30-minutes of Universal Time (UT). The vertical line(s) in each panel indicate the time at which B_Z turns southward. For all these events, there was an extended southward turning of large magnitude (> 20 nT). In

some cases, there were other southward turnings (often minor), hence two or three lines in some cases. The times are shifted by our best estimate of the velocity of the solar wind protons, as measured by the SWEPAM instrument on ACE (see for example Skoug *et al.*, 2004), plus one hour. The uncertainty of these times should be viewed as ±30 minutes.

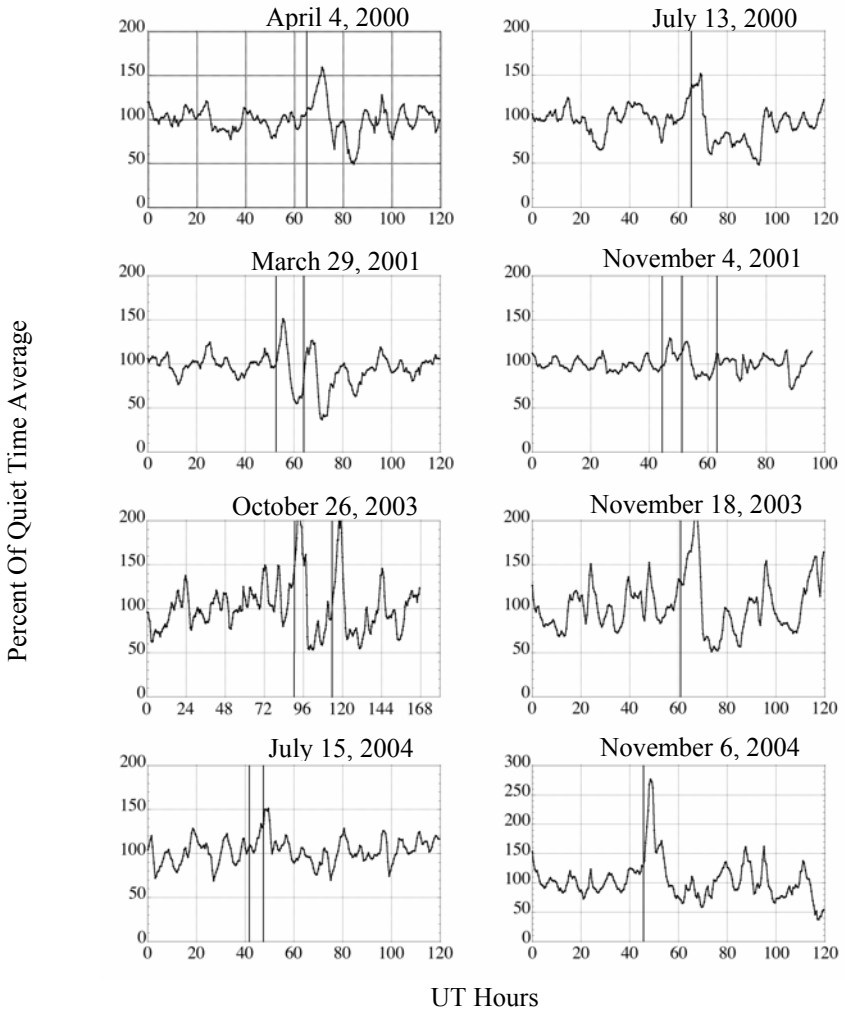

Figure 6: Average TEC change as a function of Universal Time for several events for the local time/latitude region 1200-1400 LT and ±40 degrees geomagnetic latitude, normalized to the quiet time average TEC of the 2-3 days preceding the storm event (100 = quiet time average). The vertical lines indicate times when B_Z becomes negative, as measured by the ACE spacecraft, time shifted according to the delay at which the solar wind reaches the magnetopause from ACE.

4.1 Event Discussion

All the events included here led to significant geomagnetic storms as indicated by the minimum *Dst* value reached over the storm period (column 3, table 1), except for the storm on July 17, 2004 which is interesting as a "control" case and also because major impact in the North American continent was reported (this impact is not discussed further). Except for July 2004, these storms represent the largest Dst events in the period 2000-2004. Despite the approximations inherent in the analysis due to non-uniform coverage of the ground stations, the following pattern and properties are discernable from figure 6:

1. In all these events, a TEC increase is clearly visible above the background variability in the preceding quiet days.
2. The TEC increases always begin *after* an identifiable B_Z southward turning, in some cases immediately (within one hour) of the B_Z southward event, and in other cases several hours elapse.
3. A TEC decrease is often discernable several hours (10-20) after the B_Z southward turning. The decrease will not be addressed further here.

These data suggest that B_Z southward events in the solar wind, when associated with major geomagnetic storms, are a reliable predictor of dayside TEC increases, in some cases very significant. In figure 7 we examine the correlation between the magnitude of the geomagnetic storm and the magnitude of the fractional TEC increase. The peak *Dst* value reached for the storm is plotted against the peak TEC increase relative to quiet-time average over the preceding two days. There does appear to be a general correspondence between the largest TEC increases and the largest *Dst* values, although with significant case-to-case variability. For example, *Dst* values in the range 360-380 are associated with peak TEC increases in a broad range of 63%-163%. The largest geomagnetic storm (*Dst* reaches –451 nT) is not associated with the largest TEC fractional increase, which occurred for the November 8, 2004 storm. We note that the TEC averages reported in this study must be regarded as an approximate quantity, as the true TEC average in the region studied differs from the measured values because the distribution of receivers in the region varies with Universal Time. We expect the inherent "noise" in the analysis technique is a significant contributing factor to the results in Figures 6 and 7. Nevertheless, it does appear that significant dayside TEC increases are a common feature of superstorm events.

These storms occurred at varying phases of the solar cycle, so the fractional increases occurred over highly varying quiet-time backgrounds, because of the variable ionizing solar flux which declines with solar cycle. Analysis of these events in terms of absolute TEC increase may be worth further study.

There may be several physical effects leading to the general patterns observed in figure 6. Following the interpretation of *Tsurutani et al.* (2004b), we expect that promptly penetrating electric fields from enhanced magnetospheric convection are responsible for at least some of the observed TEC increase caused by the uplift/reduced recombination mechanism mentioned earlier, particularly those that occur rapidly after B_Z southward turning. The detailed relationship between enhanced convection and magnitude of TEC increase, including pre-conditioning factors such as the ionospheric conductivity pattern possibly modulated by auroral precipitation, and the effectiveness of inner-magnetosphere shielding on the dayside, is a complex subject requiring further study and modeling.

Table 1: Event dates and times for figure 6.

Start Date	B_Z South Date	Minimum Dst Value (nT)	B_Z South Time UT hours	B_Z South Time (2)	B_Z South Time (3)
4/4/00	4/6/00	-290	17.0		
7/13/00	7/15/00	-290	16.8		
11/4/01	11/8/01	-265	20.2	3.1	15.2
3/29/01	3/31/01	-358	4.7	15.7	
10/26/03	10/29/03	-363	18.2		
10/26/03	10/30/04	-400	17.6		
11/18/03	11/20/03	-451	12.6		
7/15/04	7/17/04	-79	17.5	23.5	
11/6/04	11/7/04	-380	20.6		

For the October 2003 events, we have examined electric field data from the DMSP satellite F13 to assess whether these data reflect disturbed conditions at low latitudes. The data are shown in Figure 8 and are only available from dusk or dawn local time; we used dusk data. In figure 8a (left panel), the electric field values within ±10 degrees geomagnetic latitude measured by DMSP (SSIES) are shown for each pass, for several days starting with October

25, 2003, color coded by direction (black is westward, red is eastward). The electric field is nearly always westward until October 29 and 30, when larger eastward values appear. Figure 8b is an expanded plot centered on the storm days, showing the appearance of large eastward directed fields shortly after the B_Z south events listed in Table 1, as indicated by vertical lines. Although these electric field data are only available at dusk and not daytime, the appearance of eastward-directed fields appearing when they do is suggestive of low-latitude electrodynamic disturbance connected to solar wind conditions. (The earlier eastward field event on October 29, at ~102 hours in Figure 8a, is nearly coincident with a large but short-lived B_Z southward event at ~4 UT on October 29, which is not considered in this analysis of persistent B_Z south events).

5. Observations From Space-borne GPS

The analysis of average regional TEC in the previous section suggests that TEC increases are a common feature associated with persistent B_Z southward turnings and the resulting superstorms. The detailed spatial structure of the TEC increase is not revealed by this analysis. In this section, we use GPS receivers on a low-Earth orbiting platform (CHAMP) to provide more information on the structure of the TEC increases as a function of latitude, taking advantage of the satellite orbit to measure TEC versus latitude at the fixed local time of the orbit.

Daytime observations of the TEC above the CHAMP satellite altitude of 400 km on Oct 30 were available from the upward-viewing GPS antenna, plotted in Figure 9 (1300 local time). Slant measurements are used to estimate vertical TEC directly above the satellite as mentioned earlier. There are generally several points at a given epoch (seen as multiple traces for a single color) because there is more than one GPS satellite in view of CHAMP at elevations greater than 40 degrees. The separate traces generally agree, except for the red traces between 40 and 60 degrees latitude, which differ because of the azimuth of the raypaths to the GPS satellites: the lower TEC values are associated with a satellite being tracked in the northwest direction versus northeast/east-directed azimuths for the higher TEC values. These traces differ because of unusually large horizontal TEC gradients in the vicinity of the satellite.

Three daytime ascending passes are shown in Figure 9, the first starting within one hour of the interplanetary B_Z south event, and the two subsequent passes. The first latitudinal profile shows the typical "two-peak" structure characteristic of the quiet-time equatorial anomaly [*Hanson and Moffett,* 1966].

The next pass (red), starting at 2012 UT, measures a vastly increased TEC above CHAMP, up to 200 TECU, with the peaks farther apart. This trace begins approximately 2.75 hours after the onset of the IMF southward-B_Z event at 1736 UT. The TEC increases still further to ~350 TECU in the southern hemisphere at approximately 4 hours after the onset of the IMF southward- B_Z event (second pass after southward B_Z, shown in black). The twin peak features previously identified as an *equatorial* anomaly now appear at mid-latitudes (± 28 degrees). The ionospheric TEC above CHAMP altitudes has increased by nearly an order of magnitude (900%) at mid-latitudes (e.g. -30° geomagnetic).

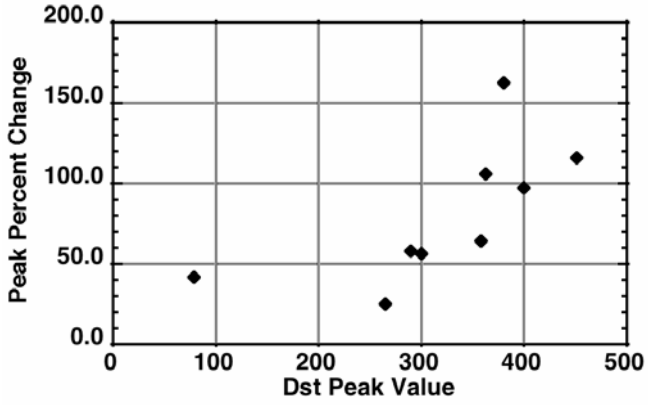

Figure 7: Peak percent TEC change in the analyzed region compared to quiet-time average of the preceding two days, for the events considered in figure 6, versus peak *Dst* excursion magni-

tude for the storm.

In Figure 9, we also plot estimated vertical TEC obtained from ground-based GPS receivers in North America (red and blue dots at 38 and 39 degrees geomagnetic latitude), for measurements located within ±6 minutes and within ±3 degrees longitude of the CHAMP location projected to the Earth's surface. Prior to the interplanetary event's impact (blue dots), the electron content above the CHAMP altitude of approximately 400 km is about half of the total electron content measured from the ground. After the interplanetary event (red dots), the fraction of electron content above CHAMP has increased significantly, suggesting more plasma resides at higher altitudes where recombination rates are reduced. This shift in the vertical plasma distribution is consistent with upward plasma drift on the dayside causing TEC increases.

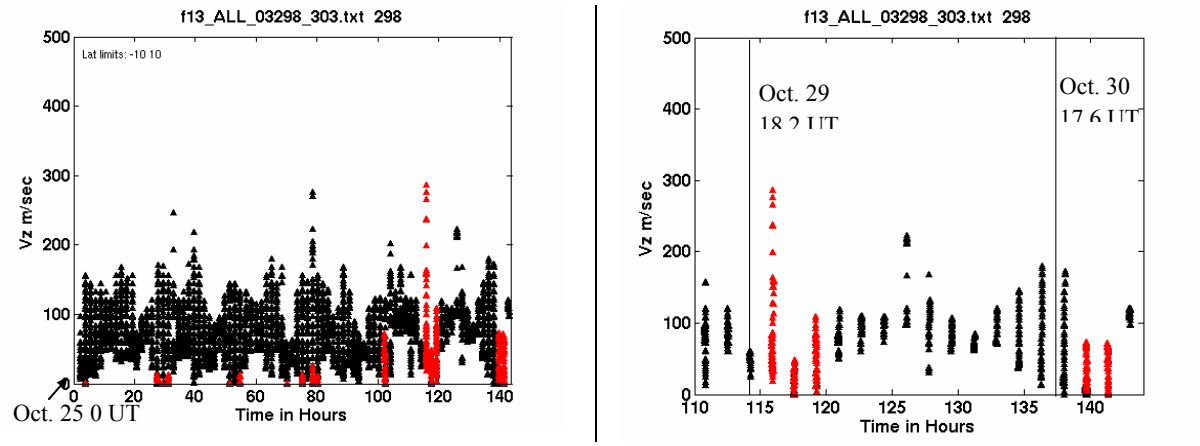

Figure 8: Electric field data from the SSIES instrument onboard the F13 DMSP satellite when the satellite was within ±10 degrees geomagnetic latitude at dusk (1745 LT). Black indicates westward fields and red eastward. The left panel shows several days of data starting with October 25, 2003, and the right panel is focused on the October 29-30, 2003 storm period. Vertical lines correspond to B_Z south event times.

Preliminary modeling results computing low to mid-latitude TEC using the NRL first-principles ionospheric model SAMI2 [Huba et al., 2000] are presented, based on a simulation study comparing observations obtained at Millstone Hill with model results during storm time conditions [Swisdak et al., 2005]. The results presented here are in qualitative agreement with the results presented in Figure 9 (assuming that the structure of electron content above CHAMP altitude is similar to total electron content structure). The purpose of the simulations is to illustrate the impact of a strong, eastward electric field and a strong equatorward neutral wind on the structure of the low- to mid-latitude ionosphere. Three simulations were performed: (1) quiet day as a benchmark, (2) strong eastward electric field and a quiet day wind, and (3) strong eastward electric field and a strong equatorward neutral wind. A simple sinusoid model of the vertical **E×B** drift at the magnetic equator is used; the peak drift speed was 40 m/s on the quiet day and 120 m/s on the storm day. These drifts correspond to peak electric fields of roughly 1.0 mV/m and 3.0 mV/m, respectively. The strong wind case imposed a strong equatorward wind (Vn = 250 m/s) at the time of peak **E×B** drift. The simulation longitude is chosen to pass over Millstone Hill (288.5° E longitude). The vertical TEC for these runs is shown in Fig. 10 for 1315 LT. The black curve denotes the quiet time simulation, the blue curve the strong eastward electric field, and the red curve the strong eastward electric field and strong equatorward wind. The imposition of a strong electric field substantially increases the vertical TEC and broadens the width of the ionization crests. Adding the strong equatorward neutral wind largely enhances the TEC but does not broaden the ionization crests significantly. These results are generally consistent with those presented in Fig. 9. The simulation results are suggestive of the physical processes responsible for the observed increase in TEC and widening of the ionization crests; in a future work we intend to perform simulation studies to be directly comparable to data.

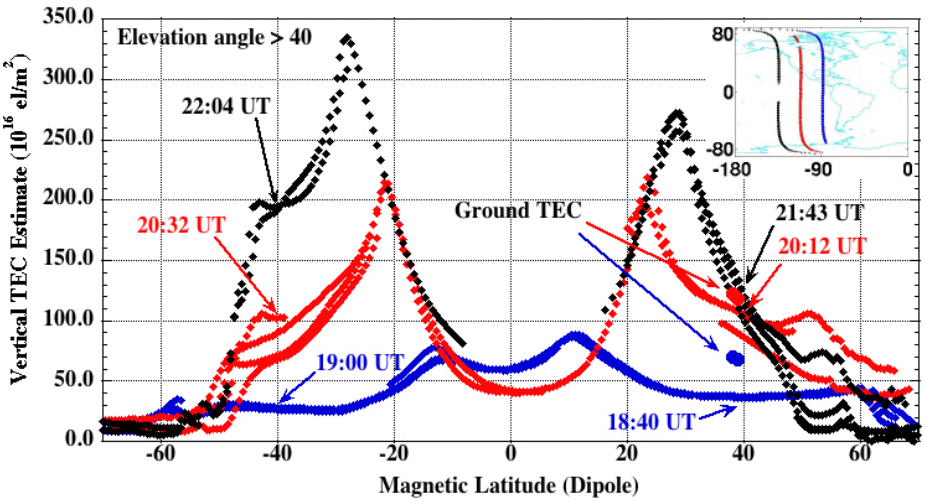

Figure 9: The super-satellite integrated electron content (IEC) as measured by the CHAMP spacecraft is shown at (blue trace) and after (red and black traces) the onset of the interplanetary event of October 30. The local time of the CHAMP orbit ranges from 1230-1330 LT for latitudes within ±60 degrees. Points missing near the anomaly trough are due to the elevation angle cut-off. The universal times of the –40 and +40 degree latitude cross-over points are shown for each trace. Also shown in the upper right are the geographical location of the traces. Total electron content averages from ground data near to the CHAMP ground track are shown as round dots.

The TEC above the CHAMP satellite for the November 7, 2004 storm is shown in Figure 11, obtained when CHAMP was in a 1400 local time orbit. The blue trace was obtained just prior to the B_z southward turning and the red and black traces are the two passes immediately following the interplanetary event after it reached the magnetopause. Additional changes are seen for this event in the next two passes (magenta and green traces). The equatorial crossing times are indicated in the figure. Before the interplanetary event, the absence of the twin-peak anomaly structure suggests that tidally generated quiet-time eastward electric fields were weak at CHAMP longitudes prior to onset. Immediately after IMF onset, TEC increases are observed without the equatorial anomaly structure. Eventually, the twin-peak anomaly structures form, resulting in widely separate peaks and large increases in mid-latitude plasma content, qualitatively similar to the October 30 event.

Plasma uplift may be creating the large TEC increases observed here, but the detailed temporal evolution of the increase appears qualitatively different than that observed on October 30, 2003. We note that the measured solar flux at 10.7 cm wavelength (UV radiance proxy) is 271.4 for October 30, 2003 versus less than half that value (124.1) for November 8, 2003. Less UV production of plasma may reduce the intensity of the daytime superfountain, which may be one factor contributing to the differences observed between the November 8, 2004 and October 30, 2003 events. The relatively long period over which electric fields appear to be acting raises questions about the effectiveness of dayside shielding for this event, if the fields originate from magnetospheric convection as we expect (see *Tsurutani et al.*, 2004b).

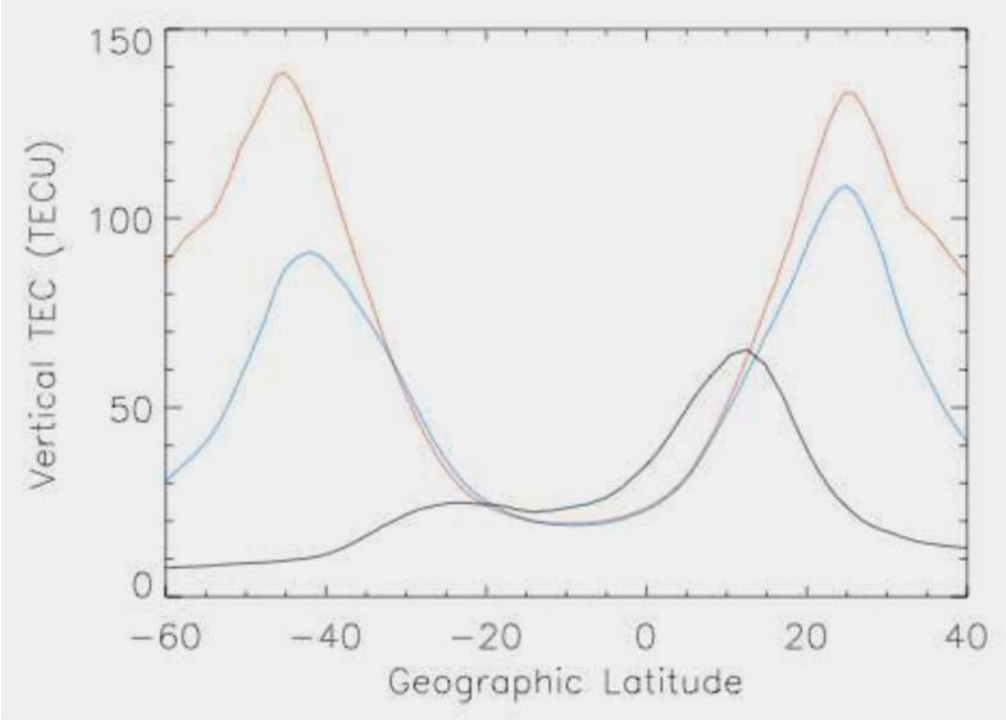

Figure 10: Modeling results comparing TEC under quiet time conditions (black), an applied sinusoidal electric field model with peak eastward field of 3 mV/m (blue), and an additional strong equatorward neutral wind (*Vn* = 250 m/s) applied at the time of peak **E×B** drift (red).

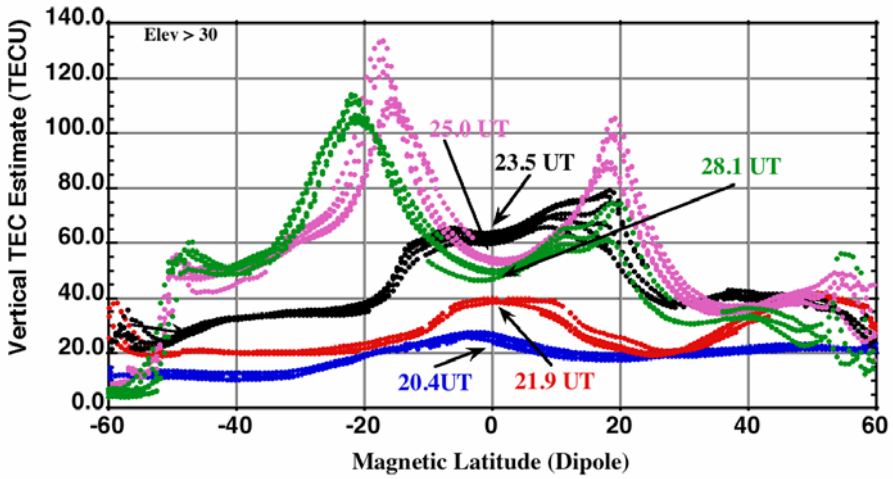

Figure 11: CHAMP observations of TEC above 400 km altitude, similar to Figure 9, for the event on November 7, 2004.

5. Conclusions

A multi-event analysis of ionospheric total electron content at low to mid-latitudes suggests that significant increases are a common response to the onset of increased interplanetary electric fields leading to superstorms. The most plausible physical mechanism for the TEC increase is prompt penetration electric fields resulting from increased magnetospheric convection and large under-shielded Region 1 currents entering the high-latitude ionosphere, causing dayside eastward directed electric fields and plasma uplift. Raising the plasma to higher altitudes decreases the average recombination rate of the plasma, while plasma production at lower altitudes due to solar pho-

tons continues unabated. The net result is a significant overall increase in daytime TEC at low to high latitudes, as a result of this "dayside super-fountain" effect. Peak TEC increases over the daytime region between ±40 degrees latitude are commonly in the range 50-200%, whereas TEC increases above 400 km altitude of nearly an order of magnitude have been observed at mid-latitudes for the Halloween storms of 2003.

The dramatic hemispheric changes reported here have major practical consequences because the overall TEC increases may intensify spatial TEC gradients and irregularity formation due to mechanisms such as Subauroral Polarization Streams (SAPS) electric fields (*Foster et al.*, 2002b), which also become intense during geomagnetic storms. Therefore, it is important to understand in more detail the physics of the daytime super-fountain and its dependence on: solar wind parameters, ionospheric and magnetosphere conditions and preconditions, and the effectiveness of inner magnetospheric shielding.

Acknowledgements

The research for this paper was performed at the Jet Propulsion Laboratory, California Institute of Technology under contract with NASA. We gratefully acknowledge the Center for Space Sciences at the University of Texas at Dallas and the US Air Force for making available the DMSP drift velocity data.

References

Abdu, M. A., I. S. Batista, G. O. Walker, J. H. A. Sobral, N. B. Trivedi, and E. R. de Paula, Equatorial ionospheric electric field during magnetospheric disturbances: local time/longitude dependences from recent EITS campaigns, *J. Atmos. Terr. Physics, 57*, p. 1065, 1995.

Anderson, D., A. Anghel, K. Yumoto, M. Ishitsuka, and E. Kudeki, Estimating daytime vertical ExB drift velocities in the equatorial F-region using ground-based magnetometer observations, Geophysical Research Letters, **29** (12), pp. 1596-1599, 2002.

Blanc, M., and A. D. Richmond, The ionospheric disturbance dynamo, *J. Geophys. Res., 85*, 1669, 1980.

Fejer, B. G., R. W. Spiro, R. A. Wolf, and J. C. Foster, Latitudinal variation of perturbation electric fields during magnetically disturbed periods: 1986 SUNDIAL observations and model results, *Ann. Geophys.*, **8**, 441, 1990.

Fejer, B. G., and L. Scherliess, Time dependent response of equatorial ionospheric electric fields to magnetospheric disturbances, *Geophys. Res. Letts., 22*, 851, 1995.

Fejer, B. G., Low latitude storm time ionospheric electrodynamics, *Journal of Atmospheric and Solar-Terrestrial Physics*, **64**, pp. 1401-1408, 2002.

Foster, J. C., P. J. Erickson, A. J. Coster, J. Goldstein and F. J. Rich, Ionospheric signatures of plasmaspheric tails, *Geophys. Res. Lett., 29(13)*, 10.1029/2002GL015067, 2002a.

Foster, J. C. and H. B. Vo, Average characteristics and activity dependence of the subauroral polarization stream, *J. Geophys. Res., 107 (A12)*, 1475, doi:10.1029/2002JA009409, 2002b.

Gonzalez, W. D. and B. T. Tsurutani, Criteria of interplanetary parameters causing intense magnetic storms (Dst < -100nT). *Planetary Space Science*, *35(9*): 1101, 1987.

Gonzalez, W. D.; Joselyn, J. A.; Kamide, Y.; Kroehl, H. W.; Rostoker, G.; Tsurutani, B. T.; Vasyliunas, V. M. What is a geomagnetic storm? *J. Geophys. Res., 99(A4*): 5771, 1994.

Hanson, W.B., and R.J. Moffett, Ionization Transport Effects in Equatorial F Region, *Journal of Geophysical Research*, **71** (23), p. 5559, 1966.

Huba, J.D., G. Joyce, and J.A. Fedder, Sami2 is Another Model of the Ionosphere (SAMI2): A new low-latitude ionosphere model, *Journal of Geophysical Research-Space Physics*, **105** (A10), pp 23035-23053, 2000.

Kamide, Y., W. Baumjohann, I.A. Daglis, W.D. Gonzalez, M. Grande, J.A. Joselyn, R.L. McPherron, J.L. Phillips, E.G.D. Reeves, G. Rostoker, A.S. Sharma, H.J. Singer, B.T. Tsurutani, and V.M. Vasyliunas, Current understanding of magnetic storms: Storm-substorm relationships, *Journal of Geophysical Research-Space Physics,* **103** (A8), pp. 17705-17728, 1998.

Kelley, M. C., J. J. Makela, J. L. Chau, and M. J. Nicolls, Penetration of the solar wind electric field into the magnetosphere/ionosphere system, *Geophys. Res. Letts., 30*, 1158, 2003.

Klein, L.W., and L.F. Burlaga, Inter-planetary magnetic clouds at 1-AU, *Journal of Geophysical Research-Space Physics*, *87* (NA2), 613, 1982.

Kozyra, J. U., V. K. Jordanova, R. B. Horne, and R. M. Thorne, Modeling the contribution of the electromagnetic ion cyclotron (EMIC) waves to stormtime ring current erosion, in Magnetic Storms, *Geophys. Monogr. Ser*., volume 98, edited by B. T. Tsurutani et al., pp. 187 – 202, AGU, Washington, D. C., 1997.

Mannucci, A.J., B.D. Wilson, D.N. Yuan, C. M. Ho, U.J. Lindqwister, T. F., Runge. A global mapping technique for GPS-derived ionospheric total electron content measurements. *Radio Science 33* (3), 565, 1998.

Mannucci, A.J., Iijima, B. A., Lindqwister, U. J., Pi, X., Sparks, L., Wilson, B.D., GPS and Ionosphere, published in *URSI Reviews of Radio Science, 1996-1999*, Oxford University Press, August 1999.

Moore A.W., A review of currently available IGS network summaries, Phys. And Chem. of the Earth – Part A, **26** (6-8), 591-594, 2001.

Nopper, R.W., and R.L. Carovillano, Polar-Equatorial Coupling During Magnetically Active Periods, *Geophysical Research Letters*, 5 (8), 699-702, 1978.

Rastogi, R.G., and J.A. Klobuchar, Ionospheric Electron-Content within the Equatorial F2 Layer Anomaly Belt, *Journal of Geophysical Research-Space Physics*, **95** (A11), pp. 19045-19052, 1990.

Reigber, C; Luhr, H; Schwintzer, P, CHAMP mission status, *Advances In Space Research*, **30** (2), pp. 129-134 2002.

Richmond, A. D., and G. Lu, Upper-atmospheric effects of magnetic storms: a brief tutorial, *J. Atmos. Solar-Terrest. Phys., 62*, 1115, 2000.

Sastri, J. H., Equatorial electric fields of the disturbance dynamo origin, *Annales Geophysicae 6*, 635, 1988.

Sastri, J. H., K. Niranjan, and K.S.V Subbarao, Response of the equatorial ionosphere in the Indian (midnight) sector to the severe magnetic storm of July 15, 2000, *Geophys. Res. Lett., 29*, No. 13, 10.1029/2002GL015133, 2002.

Scherliess, L., and B. G. Fejer, Storm time dependence of equatorial disturbance dynamo zonal electric field, *J. Geophys. Res., 102*, 24037, 1997.

Senior, C., and M. Blanc, On the control of magnetospheric convection by the spatial distribution of ionospheric conductivities, *J. Geophys. Res.*, **89**, p. 261 (1984).

Skoug, R. M., J. T. Gosling, J. T. Steinberg, D. J. McComas, C. W. Smith, N. F. Ness, Q. Hu, and L. F. Burlaga, Extremely high speed solar wind: 29-30 October 2003, J. Geophys. Res., 109, A09102, doi:10.1029/2004JA010494, 2004.

Sobral, J. H. A., M. A. Abdu, W. D. Gonzalez, I. Batista, A. L. Clua de Gonzalez, Low-latitude ionospheric response during intense magnetic storms at solar maximum, *J. Geophys. Res. 102*, 14305, 1997.

Sobral, J. H. A., M. A. Abdu, W. D. Gonzalez, C. S. Yamashita,A. L. Clua de Gonzalez, , I. Batista and C. J. Zamlutti, Responses of the low latitude ionosphere to very intense geomagnetic storms, *J. Atmos. Solar Terr. Phys., 63*, 965, 2001.

Spiro, R. W., R. A. Wolf, and B. G. Fejer, Penetration of high latitude electric field effects to low latitudes during SUNDIAL 1984, *Ann. Geophys.*, **6**, 39, 1988.

Swisdak, M., J.D. Huba, G. Joyce, and C.S-Huang, Simulation study of a positive storm phase observed at Millstone Hill, submitted to Geophys. Res. Lett., 2005.

Tanaka, T. and K. Hirao, Effects of an electric field on the dynamical behavior of the ionospheres and its application to the storm time disturbances of the F-layer, *J. Atmos. Terr. Phys., 35,* 1443, 1973.

Tsurutani, B.T., W.D. Gonzalez, F. Tang, S.I. Akasofu, and E.J. Smith, Origin of Interplanetary Southward Magnetic-Fields Responsible for Major Magnetic Storms near Solar Maximum (1978-1979), *Journal of Geophysical Research-Space Physics*, *93* (A8), 8519, 1988.

Tsurutani, B. T., W. D. Gonzalez, X. –Y. Zhou, R. P. Lepping, and V. Bothmer, Properties of slow magnetic clouds, *J. Atmosph. Solar Terr. Physics, 66*, 147, 2004a.

Tsurutani, Bruce; Mannucci, Anthony; Iijima, Byron; Abdu, Mangalathayil Ali; Sobral, Jose Humberto A.; Gonzalez, Walter; Guarnieri, Fernando; Tsuda, Toshitaka; Saito, Akinori; Yumoto, Kiyohumi; Fejer, Bela; Fuller-Rowell, Timothy J.; Kozyra, Janet; Foster, John C.; Coster, Anthea; Vasyliunas, Vytenis M., Global dayside ionospheric uplift and enhancement associated with interplanetary electric fields, *J. Geophys. Res.*, **109** (A8), p. A08302, doi 10.1029/2003JA010342, 2004b.

Vlasov, M., M.C. Kelley, and H. Kil, Analysis of ground-based and satellite observations of F-region behavior during the great magnetic storm of July 15, 2000, *Journal of Atmospheric and Solar-Terrestrial Physics*, *65* (11-13), 1223-1234, 2003.